International Journal of Pharmaceutics 410 (2011) 125–137

Contents lists available at ScienceDirect

International Journal of Pharmaceutics

journal homepage: www.elsevier.com/locate/ijpharm

Spermine grafted galactosylated chitosan for improved nanoparticle mediated gene delivery

Susan M. Alex, M.R. Rekha, Chandra P. Sharma*

Biosurface Technology Division, Biomedical Technology Wing, Sree Chitra Tirunal Institute for Medical Sciences & Technology, Poojappura, Thiruvananthapuram, Kerala 695012, India

ARTICLE INFO

Article history:
Received 1 November 2010
Received in revised form 8 February 2011
Accepted 8 February 2011
Available online 9 March 2011

Keywords:
Nanoparticle
Spermine
Endocytosis
Galactosylated chitosan
Gene delivery

ABSTRACT

Despite multitude of beneficial features, chitosan has poor water solubility and transfection ability which affect its gene delivery efficacy. The two features are improved when certain chemical modifications are incorporated into the chitosan parent backbone. This strategy is adopted here, by coupling galactose and spermine into the chitosan backbone. The conjugation was determined with FTIR and ^{1}H NMR and nanoparticle morphology was assessed by TEM and AFM techniques. Particle size, zeta potential, buffering capacity and DNA binding ability gave encouraging result of enhanced solubility and stability. *In vitro* studies of GCSM in HepG2 cell lines displayed low cytotoxicity and improved transfection. We also identified the preference of receptor mediated internalization for nanoparticles cellular uptake by treating with cellular uptake inhibitors. The results evidently led us to comprehend that galactosylated chitosan-g-spermine could be considered as a promising chitosan derivative for conducting nanoparticle mediated gene delivery.

1. Introduction

A new paradigm of gene therapy is adoption of nanotechnology to generate a suitable carrier or system, necessary to deliver the gene of interest to the site of action. The desirable vector system is examined with its possibilities that paved a broadened research into gene targeting. Concerning this, various researchers has focused on both viral and nonviral approach of vector designing. Initially, viral systems were considered for gene transfer because of its highly evolved cellular machinery to deliver genes to living cell (Verma and Somia, 1997). But clinical testing of recombinant viruses raised the potential risk of human immune system to be stimulated and the occurrence of non-specific random recombination events of viral genome with the host genome (Broeke and Burny, 2003). An alternative to this led to the invention of non viral delivery systems developed from polymers. Although polymeric vectors exhibited less efficiency in gene transfer when compared to their viral counterparts, they possessed certain attractive traits that promoted further investigation into their synthesis (Midoux et al., 2009; Morielle et al., 2008). In general, polymers, preferably ones with cationic nature are chosen due to the strong condensing ability on interaction with DNA. This would allow tight package of large amount of DNA into a compact nanosized structure that would mask the DNA from degradation (Vasir and Labhasetwar, 2007). But synthetic polymers had the disadvantage of being toxic and non degradable while natural polymers offered less toxicity and had the intrinsic property of environmental responsiveness via degradation and remodeling by cell-secreted enzymes (Dang and Leong, 2006). Hence, natural polymers with cationic property were extensively studied for nanoparticle mediated gene delivery system. And one such polymer is chitosan, first reported by Mumper et al. (1995) as a promising candidate for polymer based delivery system.

Chitosan is a copolymer of N-acetylglucosamine and glucosamine units with the presence of free amino groups that convey the amino-polysaccharide its positive charge which promote protonation even in slight acidic medium as well as favour electrostatic interaction with the phosphate groups of nucleic acids (Lai and Lin, 2009). Chitosan is regarded as a versatile polymer (Hoggard et al., 2004) in terms of its availability and cost, reduced immunogenicity, antimicrobial activity and admirable biodegradability with ecological safety. However, nascent chitosan with its high molecular weight is insoluble at neutral pH and results in viscous solution which when used as such, would perturb the flow normalcy of biological fluids (Prabaharan, 2008) that function at pH 7.4. Another issue to be concerned is its low gene expression which was found to be dependent on its various physicochemical properties (Thibault et al., 2010; Liu et al., 2007; Ishii et al., 2001). To overcome these limitations, chitosan was subjected to different chemical methodologies for creating chitosan nanoparticles that would provide

* Corresponding author.
E-mail address: sharmacp@sctimst.ac.in (C.P. Sharma).

0378-5173/$ – see front matter © 2011 Elsevier B.V. All rights reserved.
doi:10.1016/j.ijpharm.2011.02.067

enhanced solubility and transfection ability (Lai and Lin, 2009). Chemical modifications involved incorporating changes in molecular weight (Mw) (Morris et al., 2008) and degree of deacetylation (DDA) (Huang et al., 2004), conjugating with either appropriate monomers and copolymers (Wu et al., 2008; Germershaus et al., 2008) or ligands of tissue specificity (Yang et al., 2010). Though contradictory reports existed on the effect of Mw (molecular weight) and DDA (degree of deacetylation) on the transfection ability of chitosan (Lavertu et al., 2006; Huang et al., 2004; Kiang et al., 2004), there were very few reports available on chitosan of intermediate molecular weight (100–150 kDa). Hence chitosan of 120 kDa was selected by us to perform physicochemical modifications due to the presence of less data on it.

In recent times, the introduction of receptor conjugates in chitosan is widely employed to improve the transfection ability of chitosan. Adoption of carbohydrate ligands for chitosan conjugation (Il'ina and Varlamov, 2007) ensured targeted delivery in liver as they favoured affinity binding towards sugar binding receptors termed asialoglycoprotein (ASGPR) receptors found on the hepatocytes (Park et al., 2004). ASGPR allowed rapid internalization of the receptor bound ligands (Ciechanover et al., 1983), which would favour an efficient uptake of the nanoparticles. Accordingly, in our polymeric delivery system also galactose coupling was performed for selective transfection in hepatocyte derived cell lines. However, additional sugar grafting to the polysaccharide chain might cause an overall deduction in the charge positivity. This pursued us to look into an additional polyamine conjugation that may grant surface charge needed for electrostatic interactions with nucleic acids. Azzam et al. (2002) had reported the ability of polyamines to behave cationic at physiological pH and found that spermine conjugated polysaccharide was more effective in transfection. Spermine, a widely known polyamine for its role in nucleic acids, had been recently shown to enhance transfection when grafted in the anionically modified pullulan exhibiting excellent blood compatibility and *in vitro* transfection (Kanatani et al., 2006). This recommended us, for the present work, to graft the polyamine to chitosan with galactosylated modification for generating a novel polymer that might result in enhanced transfection. Along with this, the intracellular localisation of the nanoparticle, which is polymer coupled with plasmid, is also demonstrated, to find out the pathways adopted for nanoparticle mediated gene delivery.

2. Materials and methods

2.1. Materials

High molecular weight chitosan polymer (deacetylation degree, 90%) was obtained from CIFT Kochi, Spermine tetrahydrochloride, N, N′-disuccinimidyl carbonate (DSC), 4-dimethylaminopyridine (DMAP), glucosamine were purchased from Fluka. N, N-dimethylformamide (DMF) and absolute methanol was purchased from Merck, India. Lactobionic acid, branched PEI (25 K), 1-ethyl-3-(3-dimethylaminopropyl) carbodiimide hydrochloride (EDC), N-hydroxysuccinimide (NHS), fluorescein isothiocyanate (FITC), 3-(4, 5-dimethylthiazol-2-yl)-2, 5-diphenyl tetrazolium bromide (MTT), Dulbecco's modified Eagle's medium (DMEM), chlorpromazine, filipin, asialofetuin, galactose from Sigma, India. Fetal bovine serum (FBS) was from GIBCO (USA). YOYO iodide, Hoechst 33342 (Invitrogen), Calf thymus DNA (Worthington Biochemical Corp.) and pGL3 control DNA (Promega, USA). All other chemicals were of AR grade.

2.2. Depolymerisation of chitosan

Usually chitosan, purchased in bulk amounts, comes with very high molecular weight ranging between 5×10^4 Da and 2×10^6 Da which often fail to be feasible for medical applications (Mourya and Inamdar, 2008). For gene delivery purposes, chitosan either with low or intermediate molecular weight is desirous, ranging either within 30–90 kDa or within 100–150 kDa. The degree of deacetylation was not modified but the molecular weight was reduced. Reduction is obtained by oxidative degradation of chitosan with $NaNO_2$ as performed in the work of Mao et al. (2004). In brief, raw chitosan flakes was filtered through nylon membrane of pore size of 120 μm, to remove any unwanted debris and dissolved in 1% acetic acid solution. The prepared chitosan solution was reacted with 0.1 M $NaNO_2$ under constant magnetic stirring of 500 rpm, at room temperature for 3 h. The reaction mixture was subsequently neutralized with 1 N NaOH to pH 8.0 to precipitate chitosan. The precipitated chitosan was recovered by centrifugation at $3350 \times g$ for 10 min, washed thrice with deionised water, followed by two times wash with 75% methanol wash. Chitosan was then dried in vacuum oven at 60 °C for 5 h. The molecular weight was then determined using the Ubbelohde viscometer (Ventek, India).

2.3. Preparation of galactosylated chitosan with spermine coupling

To obtain galactosylated chitosan (GC), the dried chitosan was coupled with lactobionic acid in the presence of coupling agents EDC and NHS at room temperature (Kim et al., 2004). Initially 500 mg chitosan (1%) was dissolved 0.25 N HCl and stirred for 1 h. The pH was adjusted to 6.5 with 2 N NaOH and should see to that the pH does not go beyond 6.7. To this solution, lactobionic acid of 250 mg was added to chitosan, in the presence of activating agent EDC (0.1 M) and NHS (0.1 M) and kept under magnetic stirring at 500 rpm overnight. The solution was then dialyzed against distilled water for 2 days and transferred into lyophilising glass flasks. The flasks were fitted into cold vacuum based lyophiliser (LABCONO, USA) for two days to obtain moisture driven galactosylated chitosan.

The GC obtained was dissolved in mild acidic condition of 0.5% HCl (w/w) as it is insoluble in organic solvents. Further reaction was carried out in DMF, with initial dissolving of GC (0.25%) in HCl that will be 20% the total volume in DMF. GC was then activated with 6 mM DSC and 6 mM DMAP for 4 h (Kim et al., 2008). Activated GC was conjugated with spermine, added in equal amount as GC and kept for overnight stirring at 4 °C. The precipitate was recovered by acetone wash, centrifuged at $3350 \times g$ for 10 min, followed by dialysis and lyophilization. The dried product appeared to be white, thin, mesh form with paper like texture and it was coded as GCSM. The polymer was prepared in concentration 1 mg/ml MilliQ H_2O in order to be used for further experiments, unless stated otherwise. GCSM polymer (2 mg/ml) was tagged with FITC (FCP) and TRITC (TCP) (Sigma) separately for fluorescent imaging and prepared as per the manufacturers' protocol in the dye conjugation kit. FCP and TCP were then purified by dialysis using membrane of molecular weight cut off of 12,000 Da (Sigma) against distilled water.

2.4. Chemical characterization of the chitosan derivative

2.4.1. Determination of free amino groups

The free primary amino groups present in the chitosan determine the intensity of positive charge that resides in the derivatised polymer. Therefore modified chitosan was evaluated by the presence of primary amino groups that is left unreacted after the grafting reaction and this was measured using the standard procedure of a biochemical assay using TNBS (Snyder and Sobocinski, 1975). Samples were taken in 1 mg/ml concentration. GCSM was dissolved in MilliQ water, chitosan and GC chitosan in 0.5% HCl (w/w). Chemical reactions occur at the free amino group of glucosamine subunits present in chitosan and hence glucosamine was

taken as the reference, whose concentration was fixed as 100. To the sample, 200 μl 0.1% (TNBS) 2, 4, 6-trinitrobenzenesulfonic acid and 4% sodium bicarbonate was added. Triplicates were carried out for each sample and after incubation for 2 h at 37 °C, 200 μl of 2 N HCl was added to stop the reaction. Absorbance was read at 344 nm with the UV spectroscope (UV Varian Cary, USA). Results were calculated as follows:

$$\text{free amino groups } \% = \frac{\text{absorbance of sample}}{\text{absorbance of reference}} \times \text{concentration of reference } (100)$$

2.4.2. FTIR characterisation

Infrared (IR) spectra of chitosan, lactobionic acid, spermine, galactosylated chitosan and GCSM were recorded on a Fourier-transform infrared spectrometer (Shimadzu spectrophotometer). The dried samples were grounded with KBr powder and compressed into pellets for FTIR examination.

2.4.3. ^{1}H NMR analysis

^{1}H NMR spectra of GCSM, chitosan derivative was measured in D_2O using a 500 MHz spectrometer (Bruker Avance DPX 300). The analysis was performed at 22 °C and the number of transients during the measurements was set as 16. The relaxation time of the instrument during measurements was 3.17 s. All other parameters were in the default settings of the instrument as per the specifications of Bruker Avance DPX 300.

2.5. Buffering capacity

The extent of protonation of the polymer is a notable feature for the polymer to escape endosomes delivery to lysosome degradation. To study this, 6 mg of GCSM was dissolved in 30 ml MilliQ to get a final concentration of 0.2 mg/ml. At the initial stage, the pH of the polymer solution was adjusted to 10 with sodium hydroxide which was then titrated against 0.1 N hydrogen chloride, adding 50 μl gradually to record the pH changes of the polymer solution. pH profile of both branched PEI solution of 25 kDa (0.2 mg/ml), a cationic polymer reported to have the most buffering capacity and unmodified chitosan 120 kDa (0.2 mg/ml) prepared in 0.5% HCl (w/w), was also recorded to compare the buffering ability of GCSM solution.

2.6. Preparation of GCSM complexes

The dried GCSM product obtained after the modification reactions was soluble in MilliQ water. Cationic polymers showed a rapid condensation with negatively charged DNA to form compact complexes which were nanoparticles that could be also addressed as nanoplexes. GCSM was prepared in a concentration of 1 mg/ml before combining with calf thymus DNA (ctDNA). The solution was filtered through a 0.22 μm filter and kept sterile. ctDNA was also prepared in the same concentration 1 mg/ml. Nanoparticles were prepared in normal saline (NS, 0.9% sterile sodium chloride) by mixing ctDNA with varying concentration of polymer solution equivalent to DNA:polymer ratio (w/w), i.e. DNA/GCSM, expressed in terms with concentration of both ctDNA and polymer solution. ctDNA concentration is kept constant for all ratios. The system was vortexed for 15 s and incubated for 20 min at room temperature for complex formation to occur. It was made particular during complex preparation, the concentration of DNA to be constant and concentration of polymer solution to be varied to adjust the theoretical charge ratio. The complexes employed for further experiments cited below were prepared in terms of this method unless otherwise stated.

2.7. Determination of particle size and zeta potential

Nanoplexes prepared was checked for size and surface charge using the Zetasizer Nano ZS (Malvern Instruments Ltd., UK) at a temperature of 25 °C. The complexes were prepared in saline (NS, 0.9% sterile sodium chloride) with increasing DNA/polymer ratio (w/w), with ctDNA at a constant concentration of 1 mg/ml (Case et al., 2009).

The average particle size was evaluated based on dynamic light scattering phenomenon of the Zetasizer Nano ZS (Malvern Instruments Ltd., UK). The size of polyplexes was expressed as the mean diameter (*z*-average) obtained by cumulant analysis of the correlation function using the viscosity and refractive index of water in calculations (Strand et al., 2010).

Zeta potential is a function of the surface charge present on the nanoparticle and was also measured with Zetasizer Nano ZS (Malvern Instruments Ltd., UK) at a temperature of 25 °C.

2.8. Morphological analysis of GCSM nanoparticle

2.8.1. Transmission electron microscopy

The morphology of the GCSM nanoplexes were observed using TEM and the nanoparticle suspension of 10 μl, complexed at DNA/polymer ratio (w/w) of 15 was placed on a copper grid removing excess liquid with a piece of filter paper and grid was then air dried. Samples were visualized with a Hitachi 226 H 7650 instrument at 100 kV.

2.8.2. Atomic force microscopy observation

Atomic force microscopy (WITEC Confocal Raman Microscope System with Atomic Force Microscope Extension, Germany) was used for close visualization of the GCSM nanoparticle. Plasmid pLG3 was mixed with GCSM polymer solution in the DNA/polymer ratio (w/w) of 15 and was deposited on mica substrates to be operated in the contact mode of the instrument.

2.9. Gel retardation

Nanoplexes were prepared with GCSM polymer and ctDNA which was then loaded onto agarose gel to analyze the condensation ability of the polymer to retard the bound ctDNA. Increasing ratios of the GCSM nanoplexes were analysed on 1% agarose gel prepared in 1× TBE buffer (89 mM Tris–HCl pH 8.3, 89 mM borate and 2 mM EDTA), staining with 2 μl of 10 mg/ml ethidium bromide. Electrophoresis was carried out in the same buffer in a Bio-Rad electrophoresis system (Bio-Rad laboratories, CA, USA) at 100 V for 60 min. The DNA bands were then visualized and photographed using MultiImage TM Light Cabinet (Alpha Innotech Corporation, San Leandro, CA, USA). Sample ratios 6, 8, 10, 12, 14, 15, 16, 17, and 18 were considered for loading into the wells.

2.10. DNase I protection and release assay

DNase was prepared in digestion buffer containing 0.1 M sodium acetate and 5 mM magnesium sulfate at pH 7.4. Nanoplexes of varying ratios 4, 6, 8, 10, 12, 14, 15, 16, 17, and 18 were prepared. The complexes were incubated with DNase of concentration 569 U/ml. For 2 μg DNA, usually 2.28 μl of DNAse is taken. The reaction was terminated using termination buffer containing 0.5 M EDTA, 2 M NaOH and 0.5 M NaCl. Nanoplex stability was confirmed further by treating the samples with heparin of 5 μl at concentration 1000 U/ml, for 30 min. Its previously reported that heparin, a highly charged polyanion have the property to displace DNA competitively from DNA-chitosan polyplexes (Srinivasachari et al., 2007). The protection rate of GCSM polymer to retain the DNA from degradation and its release was detected by visualizing the bands run on a

1% agarose gel electrophoresis in a Bio-Rad electrophoresis system (Bio-Rad Laboratories, CA, USA).

2.11. Cell culture

The influence of GCSM nanoparticle on biological system was analysed by performing cell culture studies. The study was attempted in human liver carcinoma cell lines (HepG2) cells seeded in culture flasks with DMEM medium along with 10%FBS and incubated for 24 h at 37 °C in 5% CO_2 and 95% humidity to attain a cell growth of 80% confluency. Prior to the following culture experiments, the cells were trypsinised and transferred to multi well tissue culture plates in the density of 1×10^5 cells/well. Reports from our lab (Morris and Sharma, 2010; Rekha and Sharma, 2009) were used as reference for performing the cell culture experiments.

2.12. Cytotoxicity assay

Cell viability is a significant parameter to be evaluated in order to determine any toxic effect of the novel chitosan derivative in *in vitro* settings. The cytotoxicity was assessed by the MTT assay which contains the reagent, 3-(4, 5-dimethylthialzol-2-yl)-2.5-diphenyl tetrazolium bromide (MTT) prepared in deionised water. The trypsinised HepG2 cells, seeded into multi well tissue culture plate were kept for incubation in the same conditions of temperature and pressure. GCSM polymer corresponding to 1 mg/ml was added in triplicates at a very high concentration of 100 μg. After 24 h incubation, GCSM with the media were removed and MTT reagent (0.2 mg/ml) was added to each well. After 3 h incubation, the reagent removed and dimethyl sulfoxide (DMSO) was added to dissolve the MTT formazan crystals. Plates were incubated for 5 min and the resultant solution was measured in an automated microplate reader at 640 nm (Finstruments Microplate Reader, MTX Labs, USA). Cells in DMEM medium without GSCM sample were selected as the control to acquire viable cell measurement. Cell viability was expressed as the mean percentage of sample absorbance relative to untreated cells.

$$\text{cell viability} = \frac{\text{absorbance of sample}}{\text{absorbance of control}} \times 100$$

2.13. In vitro transfection

The harvested HepG2 cells after trypsinisation were plated onto a 4-well tissue culture plate with a density of 1×10^5 in DMEM containing 10% FBS, incubating for 24 h at 37 °C in 5% CO_2. Transfection was carried out to investigate the gene transfer efficiency of the GCSM nanoplexes. The nanoplexes were prepared, by mixing plasmid pGL3 with GCSM polymer solution in ratios of 1:15 and 1:16 and diluted rest with DMEM medium containing 10% FBS serum. These ratios showed consistent optimum size and zeta potential, and hence was selected for transfection. Nanoplexes were added to the cells and incubated at 37 °C for 4 h in 5% CO_2. Following this the nanoplexes were removed, cells further incubated with fresh medium containing serum and kept for 24 h incubation. As PEI was reported (Neu et al., 2005) to show high transfection ability, plasmid pGL3 was coupled with PEI to be used as positive control. Triplicates were carried out for the ratios and control.

The medium was then removed, followed by rinsing cells with phosphate buffered saline (PBS) and lysed with 100 μl of lysis reagent (Promega). The lysed cells were treated with luciferase assay substrate and cell extract was measured for luciferase activity expression. The relative luminance expression (RLU) was determined using the luminometer (Chamaleon, Hidex). The lysate was subjected to Micro BCA Protein Assay Reagent Kit (Pierce) for elucidating the total protein content. Gene expression efficiency was presented as percentage of observed luminance expression count to the cellular protein (mg) obtained for each sample.

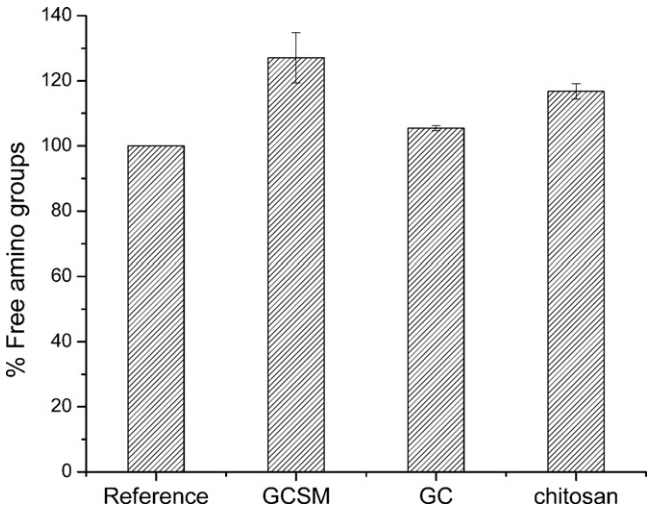

Fig. 1. TNBS assay for determination of free amino groups in GCSM, GC, chitosan with glucosamine as the reference.

2.14. Intracellular uptake studies

2.14.1. Plasmid trafficking

Plasmid DNA was tagged with YOYO as YOYO iodide is a DNA labeling dye with high sensitivity and affinity towards double-stranded DNA. The plasmid DNA was incubated for 30 min with YOYO iodide, with 2.5 μL of 10 μM YOYO labeled for 1.0 μg DNA/well. Two nanoplex combinations, in ratio 15, were made for observing plasmid trafficking. In one combination, the YOYO tagged pGL3 plasmid, was mixed with unlabelled GCSM polymer and in the other, FITC labeled GCSM was complexed with unlabelled pGL3 plasmid. After 20 min complexation, HepG2 cells were treated with the above mentioned combination of GCSM nanoparticles without the presence of any inhibitors. This also served as a control for cell uptake inhibition study. After 3.5 h the cells were treated with Hoechst 33342 for nucleus staining, followed by half hour incubation. The cells were then washed in saline, replaced with fresh media and immediately viewed under a fluorescence microscope. YOYO is reported in a recent paper to be dissociating from the plasmid DNA when transferred into the cells (Escoffre et al., 2009), which might create false appearances. To evade this, and as a control, we have treated HepG2 cells with YOYO tagged GCSM polymer alone without the presence of plasmid DNA and the same above procedure was followed.

2.14.2. Nanoplex trafficking

To further validate the intracellular distribution and unpacking of the nanoplexes, plasmid DNA tagged with YOYO as described in the above section and GCSM labeled with TRITC were complexed for cell uptake study. After 20 min complexation, HepG2 cells were treated with tagged GCSM nanoplexes. After 2.5 h the cells were treated with Hoechst 33342 for nucleus staining, followed by half hour incubation. The cells were then washed in saline, replaced with fresh media and immediately viewed under a fluorescence microscope.

2.14.3. Cell uptake studies in the presence of endocytic inhibitors

HepG2 cells were seeded to a 4-well plate and uptake study was carried out in the cells with 70% confluent growth. Nanoparticle entry inside the cell, in general, is mediated by a mechanism known as endocytosis that compile a number of trafficking channels,

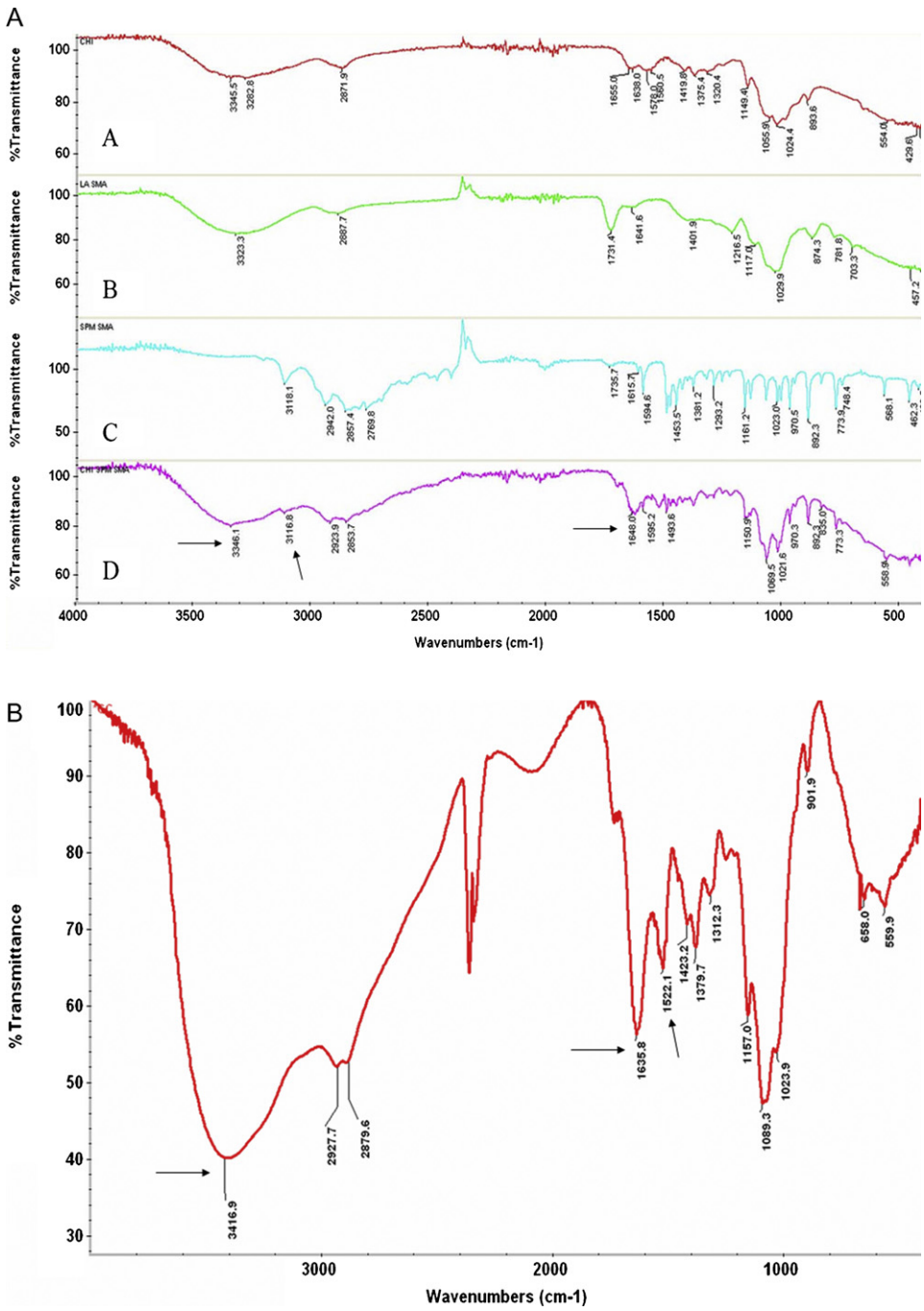

Fig. 2. Infrared spectroscopy for evaluation of chemical groups in the functional entities of the GCSM derivative. (A) FT-IR of (a) chitosan; (b) lactobionic acid; (c) spermine; (d) GCSM. (B) FT-IR of galactosylated chitosan, GC.

among which clathrin dependent, caveolae-mediated and receptor mediated internalization are prominent endocytic pathways. The intracellular movement of GCSM nanoparticle was investigated by adopting four endocytic inhibitors that is reported to cause inhibition to endocytic motion (Rejman et al., 2005; Orlandi and Fishman, 1998). To begin with, the cells were rinsed with PBS and incubated for 30 min with clathrin mediated inhibitor chlorpromazine and caveolae mediated inhibitor fillipin at a concentration of 2 μg/well and 5 μg/well, respectively (Rekha and Sharma, 2009; Kanatani et al., 2006). During the 30 min incubation, at 37 °C in 5% CO_2 pressure, the nanoplexes were prepared with FITC tagged GCSM polymer with pGL3 plasmid in the ratio 1:15. This is then followed by the removal of inhibitors containing media and cells were rinsed with fresh media. Nanoplexes tagged with FITC were added to the cells before adding the fresh media with serum for 4 h incubation. It is known, that polymeric nanoparticle with attached sugar residues is engulfed by cell through receptor mediated endocytosis. Hence, two ligands asialofeutin and glucose were added to separate wells in 1 mg/ml concentration, to study the inhibition caused by these receptor specific ligands. To the pre-treated cells, the prepared FITC labeled nanoplex ratio was added and incubated with fresh media with serum. Nucleus staining was done with Hoechst 33342. After 4 h incubation, the four inhibitor samples were subjected to twice PBS wash and the uptake mechanism inside the cell was observed using the 40× objective of fluorescence microscope (Leica DMI 3000B, Germany).

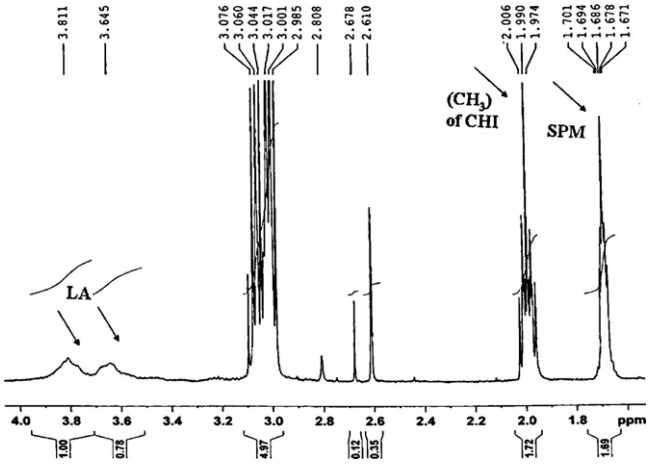

Fig. 3. ^{1}H NMR spectra of GCSM polymer.

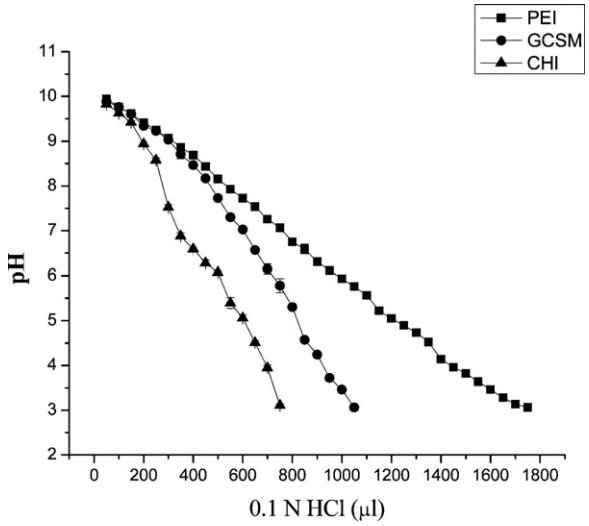

Fig. 4. Analysis of the buffering capacity of GCSM. Acid base titration of PEI, GCSM and chitosan (CHI) polymer against 0.1 N HCl. The values given are mean ± SD and $n = 3$, with standard deviation found to be very negligible.

3. Results

3.1. Chemical characterization of the chitosan derivative

Repeated depolymerisation of very high molecular weight of chitosan resulted in an intermediate range of 120–130 kDa chitosan. As the report was directed towards in achieving a chitosan derivative targeted to hepatocytes, ligand modification of the 124 kDa chitosan was carried out with lactobionoc acid to incorporate galactose groups into the chitosan backbone. Since chitosan has a p*K*a value of about 6.2–7.0, it is insoluble in neutral as well as alkaline solutions and soluble in acidic pH. But with chemical modifications (Il'ina and Varlamov, 2007), the solubility was enhanced and the recent chitosan derivative obtained was thus water soluble. The amount of free primary amino groups in depolymerised chitosan available for coupling reaction would attribute to the synthesis of several derivatives with chitosan. TNBS, a colorimetric biochemical assay determined the amount of free amino groups in chitosan, gal-chitosan (GC) and GCSM polymer. Results indicated that GC consisted of reduced free amino groups when compared to the parent compound due to the binding of galactose moiety at the reactive amino position. However, on conjugation with spermine resulted in replacing almost the reacted primary amino groups in GC by the primary groups of spermine and hence a slight increase in free amino groups is observed in the gal-chitosan-spermine derivative, GCSM as depicted in Fig. 1.

The physicochemical characterisation of GCSM was further demonstrated with FTIR and ^{1}H NMR spectroscopy. FTIR evaluation, displayed in Fig. 2A and B indicated GC and GCSM derivative of chitosan stacked with other functional groups, respectively. The IR of GC exhibited peaks at 3416 cm^{-1}, 1635 cm^{-1} and 1522 cm^{-1} whereas the final product GCSM revealed prominent peaks at 3346 cm^{-1}, 3116.8 cm^{-1} and 1648 cm^{-1}. Already a lot of previous articles have presented the ^{1}H NMR results of chitosan (Tian et al., 2003; Knight et al., 2007) and galactosylated chitosan (Jiang et al., 2007) which enabled for comparison with ^{1}H NMR of GCSM polymer. In Fig. 3, the signals at 3.811 ppm and 3.645 ppm were assigned for protons of lactobionic acid. And within 2.006–1.974 ppm, the signals corresponded to the CH_3 proton of chitosan. The signals 1.7012–1.671 ppm corresponded to protons of spermine (Ha et al., 1998). In accordance with Jintapattanakit et al. (2008), the degree of substitution of galactose and spermine was calculated to be 15% and 32%, respectively, which illustrated the successful formulation of GCSM polymer variant.

3.2. Buffering capacity of the chitosan derivative

The result shown in Fig. 4 revealed that GCSM conjugate has buffering capacity over a pH range of 10–5 against 950 μl of 0.1 N HCl titration. This was found to be slightly higher than normal buffering capacity of unmodified chitosan that showed resistance around pH 7–5 with 650 μl of the acid. PEI showed the maximum buffering capacity of pH range 10–5 with higher volume of acid titration.

3.3. Particle size measurement and zeta potential

The size of the nanoparticle is a detrimental factor to be used for gene transfer studies. The hydrodynamic diameter of the complexes indicated the size of the nanoplexes. The five ratios gave sizes of 328 nm, 258 nm, 241 nm, 241 nm, and 559 nm. Ratios 15 and 16 showed an optimum size of 241 nm generally preferred for *in vitro* studies. Nanoplexes prepared in ratios DNA/GCSM (w/w) below 12 and above 17 were very large and inconsistent, and could not be used for *in vitro* studies, hence data is not shown. The mean hydrodynamic diameter of the complexes of different weight ratios along with their zeta potential are given in Table 1. The surface charge for complexes made of varying ctDNA and GCSM ratios were found to be 10.4 mV, 11.7 mV, 13.8 mV, 7.81 mV, and 10.4 mV. Fortunately, ratios 15 and 16 showed a fairly good positive charge of 13 and 7 mV, respectively that enabled its further use.

Table 1
Particle size and zeta potential of GCSM/ctDNA nanoparticles. The values given are mean ± SD and $n = 3$.

N/P ratio	Size (nm) ± SD	Zeta potential (mV) ± SD
1:12	328 ± 8.4	10.4 ± 0.58
1:14	258 ± 35.5	11.7 ± 2.08
1:15	241 ± 33.2	13.8 ± 3.41
1:16	241 ± 28.9	7.81 ± 4.09
1:17	559 ± 158.3	10.4 ± 1.48

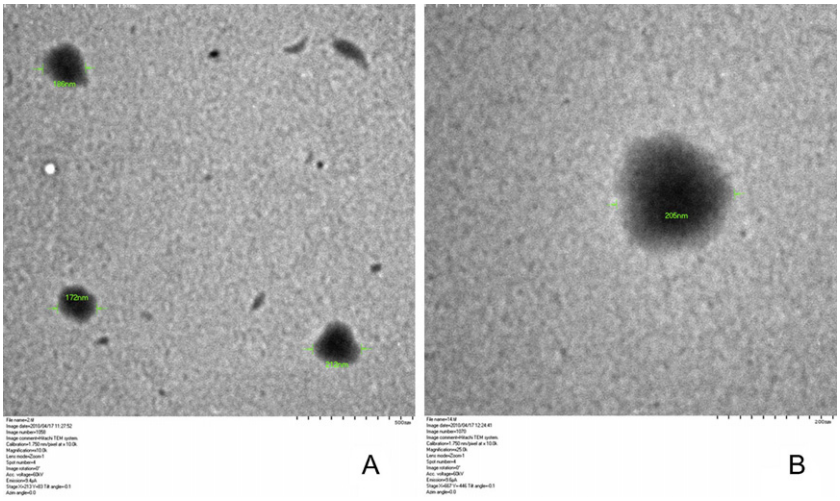

Fig. 5. TEM observation (A) GCSM nanoparticles in 1:15 ratio. (B) Single GCSM nanoparticle of 1:15 ratio.

3.4. Morphological observation

3.4.1. Transmission electron micrographs

The chitosan derivative nanoplexes did not form aggregates and distinct sizes were visualized, clearly showing the shape of the nanoparticles (Fig. 5A). Simultaneous shapes of spheroid like globular structures were seen with an average diameter of 170–215 nm. A single nanoparticle size is presented in Fig. 5B.

3.4.2. Atomic force microscopy

AFM technique was adopted to attain a surface topography image of the GCSM nanoparticle. The image (Fig. 6) further confirmed the absence of aggregates and adhesion between the nanoplexes. Distinct nanoplexes with slight irregularities were distributed and a more of ellipsoidal shape was observed, drawing a similarity in the existing kind of shapes achieved through TEM observation.

3.5. Gel retardation

The binding ability of GCSM polymer with calf thymus DNA was investigated by running agarose gel electrophoresis. GCSM nanoplexes resulted after mixing varying proportions of GCSM solution with a constant concentration of calf thymus DNA, showed no release of DNA in the lanes. The bright intensity of DNA was retained in the wells as shown in Fig. 7 which confirmed the strong interaction between the GCSM and ctDNA that retarded the movement of DNA towards the positive electrode. DNA alone without complexation was loaded in the first well resulting in a DNA smear in the first lane. And rest of the wells were loaded with the nanoplex

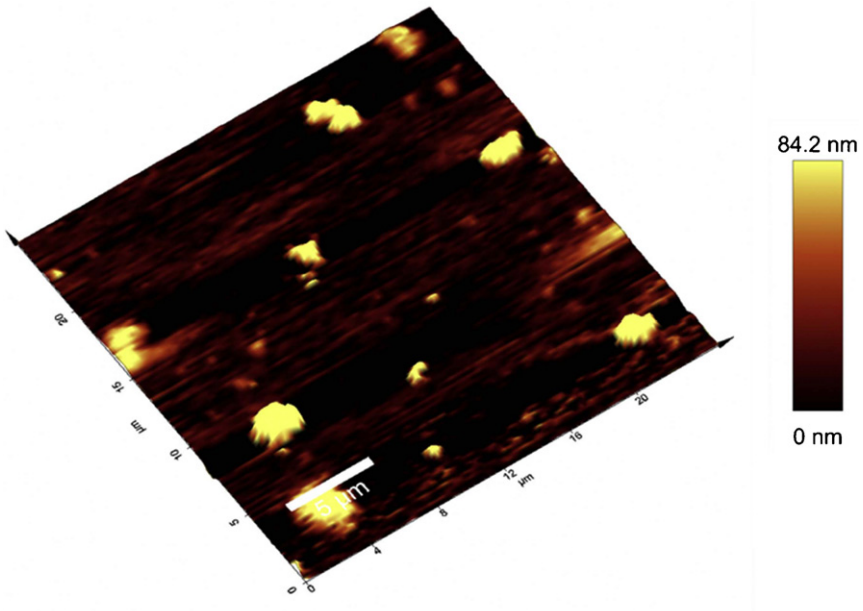

Fig. 6. AFM surface topography of GCSM nanoparticles in 1:15 ratio.

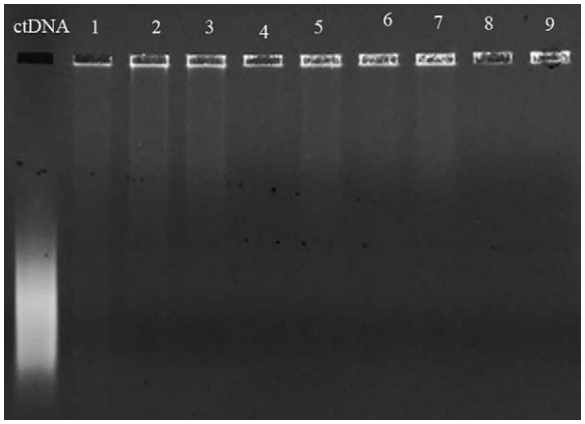

Fig. 7. Agarose gel electrophoresis performed on ctDNA/GCSM complexes. The DNA retardation ability of the nanoplex is determined. Lane ctDNA is control (2 μl DNA). Lanes 1–9 have nanoplex ratios 1:6, 1:8, 1:10, 1:12, 1:14, 1:15, 1:16, 1:17, 1:18.

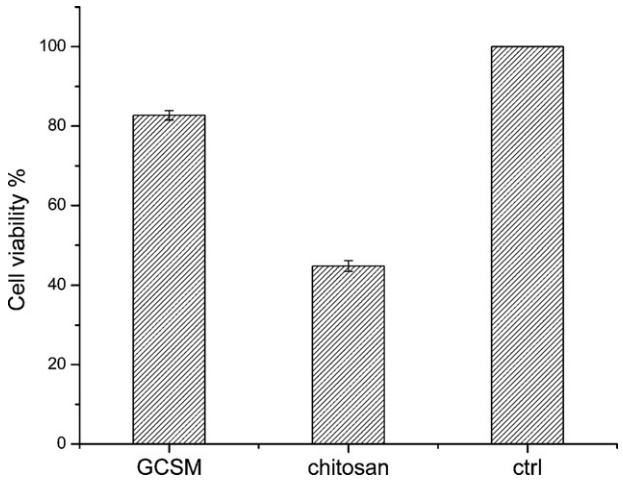

Fig. 9. Cell viability % of HepG2 cells after incubation with GCSM, chitosan and medium alone for 24 h. Cytotoxicity was evaluated by the MTT assay. The values given are mean ± SD and $n = 3$.

ratios 6, 8, 10, 12, 14, 15, 16, 17, and 18. Negligible degradation and slight DNA dissociation was observed in the ratios 6, 8, 10, 14, 15, 16 and wells with ratios 12, 17 and 18 did not show much fluorescence indicating that DNA in these ratios were degraded.

3.6. DNase I protection assay

Electrostatic interaction between DNA and the polymer need to be stable in order to obtain nanoplexes that can be consistent for a time period. Therefore, the integrity of nanoplex with ctDNA was confirmed by treating the nanoparticles with DNase for degradation study. The faint fluorescence seen in the wells. Supp. Fig. 8A indicated DNA retained in the wells which would be condensed tightly into the polymer nanosize configuration, thus protecting it from DNase attack. On treatment with heparin, the DNA was released from the bound nanoplexes as observed in Fig. 8. Ratios 4, 6, 8, 10, 12, 14, 15, 16, 17, and 18 revealed the stability of the nanoplex to remain bound to DNA. Control DNA treated with DNAse was completely degraded in its lane. Voltage fluctuations in between caused slight bend in the DNA streaks.

3.7. Cell viability

MTT assay is carried out to determine the cell viability of cells in response to the concentration of GCSM polymer. Significant cytotoxicity was not observed for GCSM in the cell lines. The % viability of GCSM polymer was compared with chitosan and control in triplicates. The graphical representation of GCSM polymer as depicted in Fig. 9, showed 80% cell viability than chitosan polymer which had cells viable below 60%. Even at high concentration of 100 μg, GCSM treated cells continued to show viability almost in comparison to the control of untreated cells.

3.8. Cell transfection

Transfection efficiency of GCSM nanoparticle was evaluated with ratios 1:16 and 1:15 combined with pGL3. Control PEI was adopted for comparison with the samples. A considerable high level of transfection in Fig. 10 was resulted with the ratios and negligible difference existed between the two ratios. Spermine coupling to galactosylated chitosan therefore attributed an efficient targeted gene expression in HepG2 cells even in the presence of serum in the medium. On other hand, ratios below the considered and higher did not provide a favourable gene expression and hence not presented here.

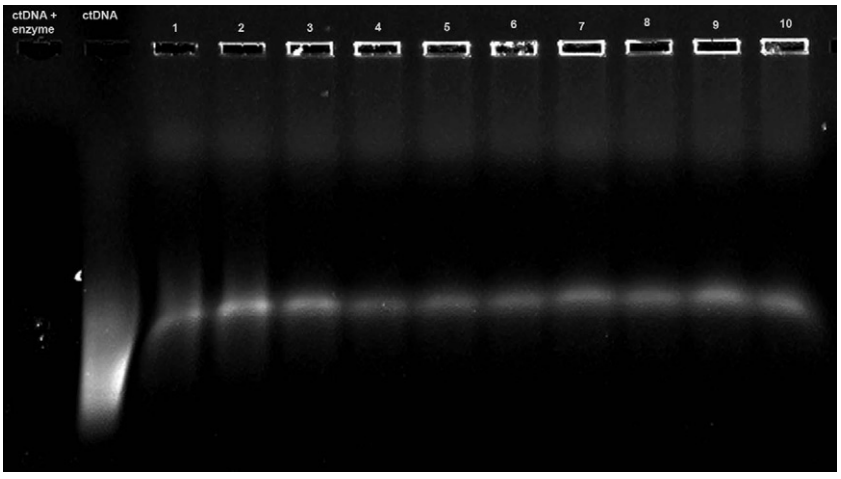

Fig. 8. DNA release showing stability of DNA with polymer GCSM after treating with DNAse and heparin. First lane is ctDNA treated with DNase followed by 2nd lane with ctDNA alone. Lanes 1–10 with ratios 1:4, 1:6, 1:8, 1:10, 1:12, 1:14, 1:15, 1:16, 1:17, and 1:18 of ctDNA/GCSM nanoparticles.

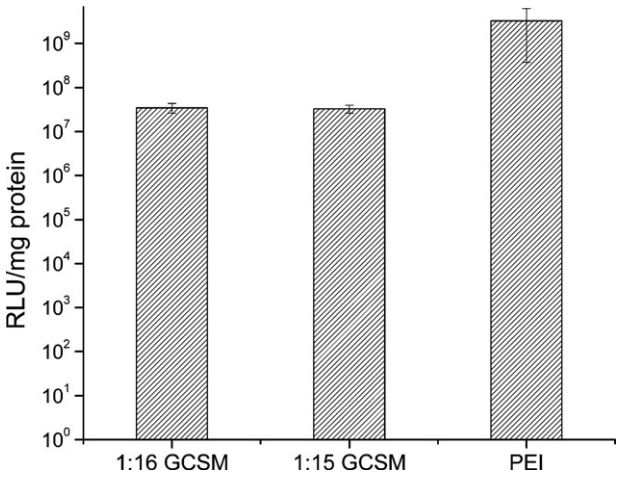

Fig. 10. Luciferase expression in HepG2 cells transfected by DNA/GCSM complexes and DNA/PEI complexes taken at two different ratios (1:15 and 1:16). The values given are mean ± SD and $n = 3$.

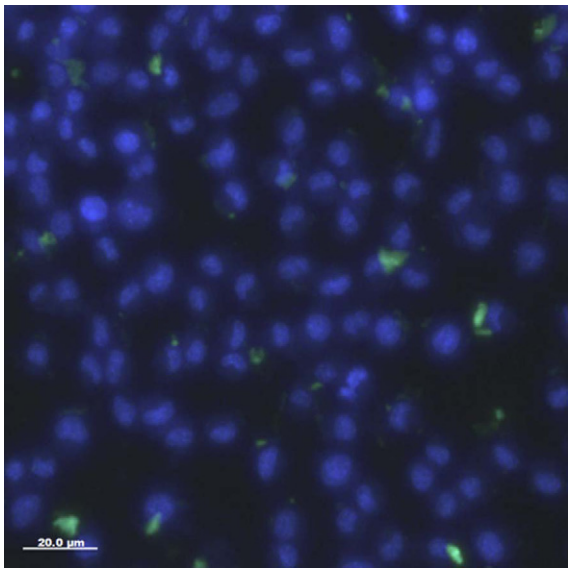

Fig. 12. FITC tagged GCSM polymer trafficking without plasmid complexation.

3.9. Plasmid trafficking and cellular uptake inhibition

Cellular internalization of YOYO labeled plasmid nanoplexes and FITC labeled nanoplexes were demonstrated in Fig. 11A and B, respectively. High distribution of the nanoplexes within the cell and nucleus was observed in both conditions, thus representing the efficient cellular uptake of the nanoplexes. In Fig. 11A, the image displayed the accumulation of FITC labeled plasmid inside the nucleus which illustrated the transfer of plasmid into the cytoplasm and finally to the Hoechst stained nucleus. As YOYO produced strong green fluorescence when bound to DNA, Fig. 11B also revealed striking green fluorescence inside the cell. Large density of fluorescent labeled nanoparticles was observed all over the Hoechst stained nucleus, indicative of the intracellular movement of the nanoparticle through the cytoplasm to the nucleus. Interestingly Escoffre et al. (2009) reported the tendency of YOYO tagged nanoplexes to give false results. Hence a control was performed for detecting the fluorescence of FITC tagged polymer alone in the absence of plasmid DNA. The image in Fig. 12 displayed fluorescence intensity more or less around the peripheral nuclear region and appeared to be weaker. The two images of tagged nanoplexes Fig. 11A and B portrayed distinctly the accumulation inside the cytoplasm and nucleus than in Fig. 12 which had very low distribution of the tagged polymer, indicating a limited entry for polymer alone into the cell. Plasmid trafficking of nanoplex with FITC tag of Figs. 11A and 12, served as control for the cell uptake inhibition study. Besides these results, the fluorescence distribution of YOYO and TRITC tagged nanoplexes were also assessed in the cells (Fig. 13). Both GCSM and plasmid DNA were found in and around

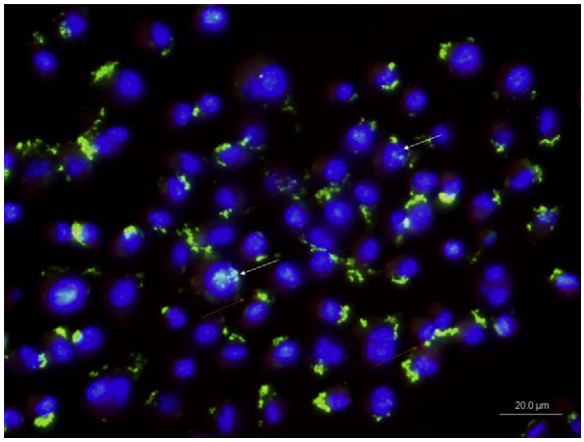

Fig. 13. Fluorescent image of cell uptake with nanoplexes comprising of YOYO tagged (green) plasmid and TRITC tagged (red) polymer with Hoechst stained (blue) nucleus. White arrows indicate the entry of gene into the nucleus and red arrows represent the polymer accumulation. (For interpretation of the references to color in this figure legend, the reader is referred to the web version of the article.)

the nucleus and the nanoplex appear to dissociate themselves in the cytoplasm. The presence of YOYO tagged gene was seen inside the nucleus with the polymer remaining more at the peripheral region of the nanoplex. The unpacking of the nanoplex facilitated the entry of YOYO tagged gene into the nucleus which may support the transfection efficiency of GCSM nanoplex. Further optimisation of multi

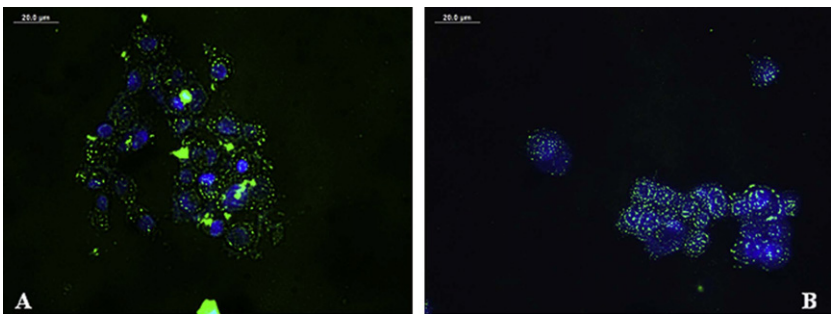

Fig. 11. Plasmid trafficking. (A) Nanoparticles with FITC tagged GCSM bound to pGL3 plasmid. (B) Nanoparticles consisting YOYO labeled pGL3 with unlabeled GCSM polymer. Both (A) and (B) serve as control for Fig. 13.

tagging of nanoplexes and unpacking mechanics is required in this study and therefore studies are continuing in this direction.

In Fig. 14A and B, the GCSM/DNA complexes were found to be localized in the nucleus of the cells, though the presence of inhibitors namely chlorpromazine and filipin were made available in the cells. On the contrary, application of ligands such as asialofeutin and galactose in Fig. 14C and D, revealed localization of nanoplexes around the peripheral regions of the nucleus. High intensity of fluorescence around the nucleus indicated a crowd of nanoparticles in the extracellular region where smooth passage of the nanoplex through the cytoplasm to the nucleus would have been hindered due to the presence of asialofeutin and galactose. This could be correlated to the likelihood of using receptor mediated pathway for the engulfment of GCSM nanoparticles. A similar observation was performed by Kanatani et al. (2006) that evaluated the uptake efficiency of pullulan-spermine based nanoplexes through endocytosis by an ASPGR.

4. Discussion

Introduction of the chemical groups into chitosan with an intermediate molecular weight range resulted in a derivative with enhanced gene expression and cellular uptake. Substitution in chitosan has now became an indispensable tool which assures enhanced transfection (Strand et al., 2010), besides designing chitosan based nanoparticles by striking an optimum balance between polyplex stability and polyplex unpacking. The incorporation of spermine and galactose in chitosan was validated by carrying out colorimetric TNBS assay. The method provided the percentage value of free amino groups and the polymer named GCSM showed a greater presence of free amino groups when compared to the parent compounds GC and chitosan. This will facilitate for the overall positive charge required for GCSM polymer to bind effectively to the nucleic acids. The IR spectra of GC and GCSM displayed the required peaks used for conjugation in chitosan. In GC derivative, lactobionic acid on reaction with chitosan resulted in hydroxyl peak at 3416 cm^{-1} along with a new amide I stretch at 1653.8 cm^{-1} and amide II stretch at 1522 cm^{-1} that clearly correlated to substitution of galactose. Subsequent conjugation of GC with spermine revealed peaks at 3116.8 cm^{-1} for amino stretch of spermine and an additional peaks at 1648 cm^{-1} was due to the C=N stretching of amide. A broad peak at 3346 cm^{-1} was due to OH stretching of parent compounds in GCSM. NMR ascertained the successful grafting of galactose and spermine into chitosan. The protons conferring high intensity peaks between 3.811 ppm and 3.645 ppm revealed the substitution of lactobionic acid groups. An increase in amino group signals between 3.07 and 2.98 ppm in the polymer was contributed from spermine and chitosan conjugation besides the specific signal at 1.07 ppm of spermine. On comparison with PEI, a highly buffering agent, GCSM polymer buffered less as seen in Fig. 4. Though being less, GCSM had far more buffering capacity than with chitosan alone. This buffering capacity was fortunately very much reasonable as, a very high buffering capacity could tend to make the polymer toxic and therefore with an optimal value of around 1200 μl 0.1 N HCl, the proton accumulation for endosome disruption could be possible.

Nanoparticle formation is the most crucial step for generating a polymeric gene carrier in which the surface charge and the average diameter of the particle size are important factors to be considered. The presence of positive and negative charges between GCSM and DNA resulted in complex coacervation. The opposite charges on the polymer complexes upon self assembly will have the overall charge rapidly neutralized till the charge becomes positive. The concentrations of GCSM and calf thymus DNA mixed at varying ratios determine the stability, integrity and charge of the nanoparticles (Strand et al., 2010). On investigation of various ratios, it was observed that the lower ratios gave rise to larger sizes with more of negative charge intensity indicating that proper condensation of the DNA with the polymer was not carried out as desired. Ratios between 12 and 17 showcased a consistent size and zeta potential within 500 nm and above 17 showed poor results in terms of both. Hence this range was focussed to obtain an optimum size and consequently ratios 15 and 16 gave a consistent size value. Though polymer concentration was quite high in these ratios, the surface charge did not get raised to very high values. Similar range of zeta potential was observed by Kim et al. (2004) who prepared nanoparticles with galactosylated chitosan and DNA. The zeta value of chitosan of molecular weight 124 kDa was 25 mV. The presence of galactose side chain deduce the charge density and sometimes it could be hypothesized that the high Mw of 124 kDa of chitosan might overweigh the less Mw of galactose and spermine resulting in an electrostatic repulsion of the ionic groups in chitosan (Chen et al., 2007) which would not allow proper packaging of nucleic acid inside. This would lead to entanglement of the rigid chain of chitosan with DNA, along with its side chains of galactose and spermine hanging loosely, thereby causing merely equilibrium of the charges. Interestingly, this type of polyplex condensation are governed by two concomitant effects known as “re-entrant condensation” and “charge inversion”, where increase in polyion content has hardly any effect on the overall charge distribution on the nanoplex (Bordi et al., 2007). However, at times only a slight positive charge is preferred over very high surface charges for cell culture studies, as previous reports (Germershaus et al., 2008) showed the chances of cytotoxicity when the amount of amino groups were increased. This confirmed the relationship between high charge density and toxicity (Lv et al., 2006). The surface charge of naked ctDNA came around −17.9, whereas the surface charge for complexes made of varying GCSM and ctDNA ratios was found to range from 10 to 13 mV, which was obviously a desirable cationic charge to mediate transfection. As ratio 15 had a slight higher zeta when compared to the other ratios, nanoplex of this particular ratio was considered along with its optimum size for our later experiments.

Particle size plays an important role in transferring genes to the cells and we tried to obtain nanoparticles of size within 250 nm range to facilitate the uptake of the particles. The morphological observation by TEM displayed a distorted spherical shape with a size distribution slightly smaller than that measured by the Zetasizer. A similar observation occurred for Chen et al. (2007) and it is likely that dried nanoparticles were used in TEM experiment while in Zetasizer the particles were analysed in liquid dispersion. As chitosan possessed inherent swelling property, GCSM would be expected to swell in suspension which would result in a large hydrodynamic size when measured by the Zetasizer. The shape has been more or less of globular which depict that the shape is resulted in order to strike the balance between packaging stability and intracellular disassembly of complexes (Strand et al., 2010; Reitan et al., 2009). The surface images obtained from AFM also supported the TEM size images, clearly displaying the distinct boundary of each nanoparticle without any aggregation. Both TEM and AFM images emphasized the formation of spheroid shapes of the nanoparticle created due to the localized bending or distortion of GCSM when bound to ctDNA. These kind of shapes for chitosan based DNA nanoparticles acquired from TEM and AFM had been noticed in other few report too (Zhang et al., 2008).

The integrity of the nanoparticle to remain stable in biological system is one of the parameters that need to be elucidated. And for this the electrophoretic mobility of the nanoparticle was analysed which clearly showed the retardation movement of DNA, hardly passing out from the wells. The bands are bright and luminescent stating that GCSM polymer was able to constrict DNA,

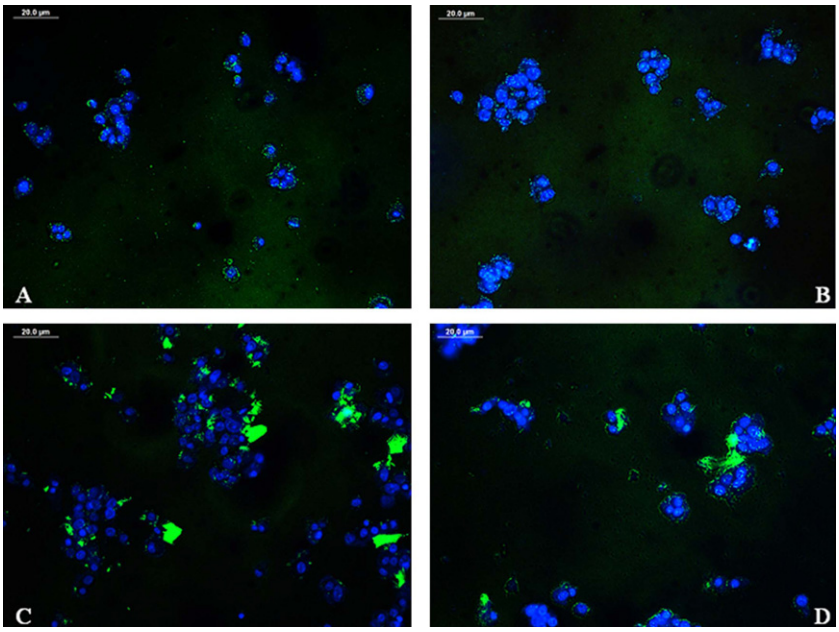

Fig. 14. Fluorescent images of cell uptake study with inhibitors. These inhibitors are specific to the various endocytic pathways that regulate nanoplex entry into the cell. (A) Chlorpromazine; (B) filipin; (C) asialofeutin; (D) galactose.

hence over shielding it from the attack of any enzymes. This was further validated by applying DNase treatment on nanoparticles in which the figure showed certain fluorescent DNA fragments in the wells. Despite the presence of the nuclease, GCSM polymer was able to protect ctDNA from enzyme digestion. On heparin displacement of DNA from the complexes, the lanes revealed the presence of DNA smear as same as the lane showing enzyme untreated control DNA. A trail of faint diffusion of fluorescence was also detected which imparts to the leaching of small amounts of DNA degradation or loosely bound sheared DNA strands from the nanoparticles. The control well without any fluorescence appeared to have their DNA completely degraded. Hence, the ratios conferred the integrity of GCSM nanoparticle.

GCSM-DNA nanoparticles succeeded in showing resistance to nuclease attack but the ability of the polymer to either evade from the endo-lysosomal pathway or escape from the endosome is another necessity for efficient cellular gene uptake to take place. The hypothesis related to proton buffering capacity for certain polymers remark the capability of a polymer that is engulfed inside an endosome (Mintzer and Simanek, 2009) to disrupt the membranes by causing differences in pH prevailing both inside and outside of vesicle. In general, the polyplexes are directed into the endosome wherein the amino groups present on the GCSM polymer tend to enhance the positive charge within the vesicle and this accumulation of a single charge will create a whole imbalance in the endosome leading to its swelling and disruption (Lai and Lin, 2009). GCSM polymer was observed to show more buffering nature than unmodified chitosan which would facilitate the release of nanoparticles into the cytoplasm that could be subsequently sequestered towards the nucleus by yet to be discovered mechanisms.

It is considered that an ideal polycationic nanoparticle should protect the DNA bound to it from extracellular barriers, penetrating through the cell membranes followed by endosomal escape and into the nucleus for genome insertion (Azzam et al., 2002). Finally, it should be biodegraded and eliminated from the cell and tissue without causing toxicity (Huang et al., 2004), a vital perspective that needs to be reckoned with before therapeutic administration of polyplexes. Literature evidence cited that chitosan (Erbacher et al., 1998) showed negligible level of toxicity and even with further vector modifications on this parent polymer, the viability of the cells remains unchanged. In addition, hepatocyte targeting galactosylated chitosan gene carriers conjugated with PEI (Kim et al., 2005) and pullulan-spermine based nanoparticles (Thakor et al., 2009) also reported low cytotoxicity. Hence, GCSM nanoparticle having chemical combinations of galactose and spermine on the parent chitosan backbone demonstrated up to 80% of cell viability supporting the above reports.

On introducing derivatives into chitosan, the transfection efficiency of chitosan in several reports has shown enhancement. Similarly, the novel approach of modification in chitosan employing galactose and spermine also revealed a considerable increase in gene transfer. The efficiency was evaluated with aid of the luciferase assay, a more sensitive method than fluorescence intensity determination. Nanoparticles were taken in two ratios in terms of its fair positive surface charge and optimum nano size that govern the feasibility of any nanoparticle to effect cell uptake (Kunath et al., 2003). On comparison with PEI 25 kDa control which is known to be a highly effective cationic gene vector, the transfection efficiency of GCSM vector is measured. Between the two ratios, transfection seemed to be slightly higher in the lower ratio which may confer that the polymer at that particular DNA/polymer (w/w) ratio was able to provide a dense condensation of DNA. There were pioneer experiments on transfection efficiency of chitosan based on parameters defining the pH of the transfection media, amine to phosphate ratio (N/P) and the amount of pDNA optimized for nanoparticle preparation (Sato et al., 2001; Huang et al., 2004; Thakor et al., 2009). In these earlier reports the involvement of serum in the media did not cause any inhibition in transfection mediated by chitosan nanoparticles and hence the entire cell culture studies for GCSM nanoparticles were carried out in presence of 10% FBS. The results were also complementing to the fact that serum had very little detrimental effect on transfection when glycosylated chitosan is

adopted for nanoparticle formation (Sato et al., 2001, Srinivasachari et al., 2006).

The potential of liver targeted gene delivery is one of the major concerns for developing an efficient nanoparticle for gene transfer. Liver is susceptible to many disease states like hepatoma carcinoma which need to be addressed (Nguyen and Ferry, 2004) and its accessibility to the entire organ system by systemic circulation has invited attention for therapeutic gene delivery. Efficient gene transfer into the HepG2 cells should therefore demonstrate a complete internalization of the nanoparticle inside the cell. The transfer of gene by the nanoplex to nucleus is identified by YOYO iodide labeling of the plasmid that enabled its fluorescent microscopic observation. Although YOYO iodide was recently argued to be not an effective marker for studying intracellular trafficking (Escoffre et al., 2009), the fluorescent intensity produced by this dye was far exceeding than compared to other covalent dyes. YOYO also featured high binding affinity to dsDNA and when unbound to DNA, it exhibited extremely low fluorescence level. The dye was not affected by pH which made it more attractive than fluorescein which might be affected by pH changes in tissues (Perry et al., 2008). Polyplex labeled with FITC was adopted for cell uptake experiment without any inhibitor treatment and that was used to for comparison for both intracellular inhibition studies and plasmid trafficking. A report by Rekha and Sharma (2009) using pullulan-spermine also showed a similar result of high localization of plasmid DNA in and around the nucleus which can be attributed to the chances of effective gene transfer. Therefore with the prevailing GCSM nanoparticle also, a fairly large amount of hoarding of plasmid in and around the nucleus delivered by the nanoparticle reflected the efficient transfection result that was obtained. Disassembly of the nanoplexes is a mandatory need to allow the gene of interest to enter the nucleus. Elucidation of nanoplex disassociation before or after the nuclear entry is vaguely reported, though Kanatani et al. (2006) have attempted to show nanoplex unpacking. In the same report, spermine has been used in conjugation for polymer derivitisation and hence a similar attempt was demonstrated by us with spermine conjugated galactosylated chitosan to investigate nanoplex disassembly during cell uptake. Distinct localisation of tagged plasmid DNA was observed at the nuclear regions with faint presence of tagged polymer remaining in the cytosol region. But further investigation is required to acquire an in-depth observation of nanoplex unpacking.

Uptake is mediated by the different pathways of the endocytosis mechanism (Rejman et al., 2005) and each inhibitors of the distinct pathway were used for investigating the actual pathway that would be likely to be adopted by GCSM nanoparticle for its internal trafficking in the cytoplasm. HepG2 cells were treated with inhibitors namely chlorpromazine, filipin and asialofetuin that were known to inhibit the clathrin, caveolae and ASPGR mediated endocytosis, respectively. The nanoparticle ratio that showed enhanced transfection was adopted for the internal localization of FITC labeled polymer. It was observed that the inhibitors of clathrin and caveolae did not prevent GCSM nanoparticle from entering the cell clearly stating that GCSM nanoparticles do not pursue the above two pathways for its trafficking process. On the contrary, the application of ligands such as asialofeutin and glucose as inhibitors revealed a marked reduction in the distribution of GCSM nanoparticles. Accumulation of GCSM nanoplexes more or less around the perinuclear region of the Hoechst stained nucleus indicated that receptor mediated endocytosis is the much preferred pathway for cellular entry, when compared to the other two mentioned pathways. Receptor mediated uptake would be of advantage for further affirmation of GCSM nanoparticle for efficient gene transfer, as receptor mediated endocytosis (RME) allowed a more rapid means of ligand targeted internalization compared to that of untargeted complexes, providing a prospect for appropriate selection of targeting ligands and controlled delivery into the intracellular trafficking pathway (Jones et al., 2003).

5. Conclusion

Chitosan based delivery system is still an attractive polymer due to its biodegradable nature and biocompatibility which would replace the toxic effect of other synthetic polymers on living cells. GCSM nanoparticle exhibited solubility and enhanced transfection that is found lacking in chitosan without modifications. Here, galactose conjugation in chitosan coupled with spermine, facilitated preferential gene transfer to the liver cells. It is also likely that depolymerised chitosan with a molecular weight in the intermediate range seemed a better parent backbone for chemical conjugation that executed transfection and intracellular uptake for transgene expression. The promising chitosan derivative should be further analysed with confocal and flow cytometry to gain a better perspective of the intracellular trafficking and colocalisation of the nanoparticles.

Acknowledgements

This work was supported by the Department of Science & Technology, Govt. of India through the project 'Facility for nano/microparticle based biomaterials - advanced drug delivery systems' #8013, under the Drugs & Pharmaceuticals Research Programme. We express our thanks to Dr. H.K. Varma for IR faculty and Dr. Annie John, SCTIMST for TEM studies. Thanks are due to Director and Head for providing facility.

Appendix A. Supplementary data

Supplementary data associated with this article can be found, in the online version, at doi:10.1016/j.ijpharm.2011.02.067.

References

Azzam, T., Raskin, A., Makovitzki, A., Brem, H., Vierling, P., Lineal, M., Domb, A.J., 2002. Cationic polysaccharides for gene delivery. Macromolecules 35, 9947–9953.
Bordi, F., Cametti, C., Sennato, S., Viscomi, D., 2007. Radiofrequency dielectric loss relaxation in polyion-induced liposome aggregates. J. Colloid Interface Sci. 309, 366–372.
Broeke, A.V.D., Burny, A., 2003. Retroviral vector biosafety: lessons from sheep. J. Biomed. Biotechnol. 1, 9–12.
Casé, A.H., Picola, I.P.D., Zaniquelli, M.E.D., Fernandes, J.C., Taboga, S.R., Winnik, F.M., Tiera, M.J., 2009. Physicochemical characterization of nanoparticles formed between DNA and phosphorylcholine substituted chitosans. J. Colloid Interface Sci. 336, 125–133.
Ciechanover, A., Schwartz, A.L., Lodish, H.F., 1983. Sorting and recycling of cell surface receptors and endocytosed ligands: the asialoglycoprotein and transferrin receptors. J. Cell. Biochem. 23, 107–130.
Chen, Y., Mohanraj, V.J., Wang, F., Benson, H.A.E., 2007. Designing chitosan–dextran sulfate nanoparticles using charge ratios. AAPS Pharm. Sci. Tech. 8, E1–E9.
Dang, J.M., Leong, K.W., 2006. Natural polymers for gene delivery and tissue engineering B. Adv. Drug Deliv. Rev. 58, 487–499.
Erbacher, P., Zou, S., Bettinger, T., Steffan, A.M., Remy, J.S., 1998. Chitosan-based vector/DNA complexes for gene delivery: biophysical characteristics and transfection ability. Pharm. Res. 15, 1332–1339.
Escoffre, J.-M., Bellard, E., Golzio, M., Teissi, J., Rols, M.P., 2009. Transgene expression of transfected supercoiled plasmid DNA concatemers in mammalian cells. J. Gene Med. 11, 1071–1073.
Germershaus, O., Mao, S.R., Sitterberg, J., Bakowsky, U., Kissel, T., 2008. Gene delivery using chitosan, trimethyl chitosan or polyethylenglycol-graft-trimethyl chitosan block copolymers: establishment of structure–activity relationships in vitro. J. Control. Release 125, 145–154.
Ha, C.H., Sirisoma, N.S., Kuppusamy, P., Zweier, J.L., Woster, P.M., Casero, J.R.R.A., 1998. The natural polyamine spermine functions directly as a free radical scavenger. Proc. Natl. Acad. Sci. U.S.A. 95, 11140–11145.
Hoggard, K.M., Varum, K.M., Issa, M., Danielsen, S., Christensen, B.E., Stokke, B.T., Artursson, P., 2004. Improved chitosan-mediated gene delivery based on easily dissociated chitosan polyplexes of highly defined chitosan oligomers. Gene Ther. 11, 1441–1452.

Huang, M., Khor, E., Lim, L.-Y., 2004. Uptake and cytotoxicity of chitosan molecules and nanoparticles: effects of molecular weight and degree of deacetylation. Pharm. Res. 21, 344–353.
Il'ina, A.V., Varlamov, V.P., 2007. Galactosylated derivatives of low-molecular-weight chitosan: obtaining and properties. Appl. Biochem. Microbiol. 43, 82–87.
Ishii, T., Okahata, Y., Sato, T., 2001. Mechanism of cell transfection with plasmid/chitosan complexes. Biochim. Biophys. Acta 1514, 51–64.
Jiang, H.-L., Kwon, J.T., Kim, Y.-K., Kim, E.-M., Arote, R., Jeong, H.-J., Nah, J.-W., Choi, Y.-J., Akaike, T., Cho, M.-H., Cho, C.S., 2007. Chitosan-graft-polyethylenimine as a gene carrier. Gene Ther. 14, 1389–1398.
Jintapattanakit, A., Maob, S., Kissel, T., Junyaprasert, V.B., 2008. Physicochemical properties and biocompatibility of N-trimethyl chitosan: effect of quaternization and dimethylation. Eur. J. Pharm. Biopharm. 70, 563–571.
Jones, A.T., Gumbleton, M., Duncan, R., 2003. Understanding endocytic pathways and intracellular trafficking: a prerequisite for effective design of advanced drug delivery systems. Adv. Drug. Deliv. Rev. 55, 1353–1357.
Kanatani, I., Ikai, T., Okazaki, A., Jo, J., Yamamoto, M., Imamura, M., Kanematsu, A., Yamamoto, S., Ito, N., Ogawa, O., Tabata, Y., 2006. Efficient gene transfer by pullulan–spermine occurs through both clathrin- and raft/caveolae-dependent mechanisms. J. Control. Release 116, 75–82.
Kiang, T., Wen, J., Lim, H.-W., Leong, K.W., 2004. The effect of the degree of chitosan deacetylation on the efficiency of gene transfection. Biomaterials 25, 5293–5301.
Kim, T.K., Kim, S.I., Akaike, T., Cho, C.S., 2005. Synergistic effect of poly (ethylenimine) on the transfection efficiency of galactosylated chitosan/DNA complexes. J. Control. Release 105, 354–366.
Kim, E., Lee, B.S., Pyo, H.-B., Song, H.-W., Kim, Y.-P., Choi, I.S., Kim, H.-S., 2008. Fabrication of nonbiofouling surface and its application to surface plasmon field-enhanced fluorescence spectroscopy. Biochip J. 2, 103–110.
Kim, T.H., Park, I.K., Nahb, J.W., Choia, Y.J., Choa, C.S., 2004. Galactosylated chitosan/DNA nanoparticles prepared using water-soluble chitosan as a gene carrier. Biomaterials 25, 3783–3792.
Knight, D.K., Shapka, S.N., Amsden, B.G., 2007. Structure, depolymerization, and cytocompatibility evaluation of glycol chitosan. J. Biomed. Mater. Res. A 83A, 787–798.
Kunath, K., Harpe, A.V., Fischer, D., Petersen, H., Bickel, U., Voigt, K., Kissel, T., 2003. Low-molecular-weight polyethylenimine as a non-viral vector for DNA delivery: comparison of physicochemical properties, transfection efficiency and in vivo distribution with high-molecular-weight polyethylenimine. J. Control. Release 89, 113–125.
Lai, W.-F., Lin, M.C.-M., 2009. Nucleic acid delivery with chitosan and its derivatives. J. Control. Release 134, 158–168.
Lavertu, M., Meĭthot, S., Tran-Khanh, N., Buschmann, M.D., 2006. High efficiency gene transfer using chitosan/DNA nanoparticles with specific combinations of molecular weight and degree of deacetylation. Biomaterials 27, 4815–4824.
Liu, X., Howard, K.A., Donga, M., Andersen, M.O., Rahbek, U.L., Johnsen, M.G., Hansen, O.C., Besenbachera, F., Kjems, J., 2007. The influence of polymeric properties on chitosan/siRNA nanoparticle formulation and gene silencing. Biomaterials 28, 280–1288.
Lv, H.T., Zhang, S.B., Wang, B., Cui, S.H., Yan, J., 2006. Toxicity of cationic lipids and cationic polymers in gene delivery. J. Control. Release 114, 100–109.
Mao, S., Shuai, X., Unger, F., Simon, M., Bi, D., Kissel, T., 2004. The depolymerization of chitosan: effects on physicochemical and biological properties. Int. J. Pharm. 281, 45–54.
Midoux, P., Pichon, C., Yaouanc, J.-J., Jaffrès, P.-A., 2009. Chemical vectors for gene delivery: a current review on polymers, peptides and lipids containing histidine or imidazole as nucleic acids carriers. Br. J. Pharmacol. 157, 166–178.
Mintzer, A.M., Simanek, E.E., 2009. Nonviral vectors for gene delivery. Chem. Rev. 109, 259–302.
Morielle, M., Passirani, C., Vonargbourg, A., Claavreul, A., Benoit, J.-P., 2008. Progress in developing cationic vectors for non viral systemic gene therapy against cancer. Biomaterials 29, 3477–3496.
Morris, V.B., Neethu, S., Abraham, T.E., Pillai, C.K.S., Sharma, C.P., 2008. Studies on the condensation of depolymerized chitosans with DNA for preparing chitosan-DNA nanoparticles for gene delivery applications. J. Biomed. Mater. Res. B: Appl. Biomater., 282–292.
Morris, V.B., Sharma, C.P., 2010. Folate mediated histidine derivative of quaternised chitosan as a gene delivery vector. Int. J. Pharm. 389 (1–2), 176–185.
Mourya, V.K., Inamdar, N.N., 2008. Chitosan-modifications and applications: opportunities galore. React. Funct. Polym. 68, 1013–1051.
Mumper, R.J., Wang, J.J., Claspell, J.M., Rolland, A.P., 1995. Novel polymeric condensing carriers for gene delivery. Proc. Int. Symp. Control. Release Bioactive Mater. 122, 178–179.
Neu, M., Fischer, D., Kissel, T., 2005. Recent advances in rational gene transfer vector design based on poly (ethyleneimine) and its derivatives. J. Gene. Med. 7, 992–1009.
Nguyen, T.H., Ferry, N., 2004. Liver gene therapy: advances and hurdles. Gene Ther. 11 (Suppl. 1), S76–84.
Orlandi, P.A., Fishman, P.H., 1998. Filipin-dependent inhibition of cholera toxin: evidence for toxin internalization and activation through caveolae-like domains. J. Cell Biol. 141, 905–915.
Perry, H.A.D., Amer, F., Saleh, A., Aojula, H., Pluen, A., 2008. YOYO as a dye to track penetration of LK15 DNA complexes in spheroids: use and limits. J. Fluoresc. 18, 155–161.
Park, I.K., Jiang, H.L., Cook, S.E., Cho, M.H., Kim, S.I., Jeong, H.J., 2004. Galactosylated chitosan (GC)-raft-poly (vinyl pyrrolidone) (PVP) as hepatocyte-targeting DNA carrier: in vitro transfection. Arch. Pharm. Res. 27, 284–289.
Prabaharan, M., 2008. Chitosan derivatives as promising materials for controlled drug delivery. J. Biomater. Appl. 23, 4–36.
Reitan, N.K., Maurstad, G., Davies, C.de.L., Strand, S.P., 2009. Characterizing DNA condensation by structurally different chitosans of variable gene transfer efficacy. Biomacromolecules 10, 1508–1515.
Rejman, J., Bragonzi, A., Conese, M., 2005. Role of clathrin- and caveolae-mediated endocytosis in gene transfer mediated by lipo- and polyplexes. Mol. Ther. 12, 468–474.
Rekha, M.R., Sharma, C.P., 2009. Blood compatibility and in vitro transfection studies on cationically modified pullulan for liver cell targeted gene delivery. Biomaterials 30, 6655–6664.
Sato, T., Ishii, T., Okahata, Y., 2001. In vitro gene delivery mediated by chitosan. Effect of pH, serum and molecular mass of chitosan on the transfection efficiency. Biomaterials 22, 2075–2080.
Snyder, S.L., Sobocinski, P.Z., 1975. An improved 2, 4, 6-trinitrobenzenesulfonic acid method for the determination of amines. Anal. Biochem. 64, 284–288.
Srinivasachari, S., Liu, Y., Prevette, L.E., Reineke, T.M., 2007. Effects of trehalose click polymer length on pDNA complex stability and delivery efficacy. Biomaterials 28, 2885–2898.
Srinivasachari, S., Liu, Y.M., Zhang, G.D., Prevette, L., Reineke, T.M., 2006. Trehalose click polymers inhibit nanoparticle aggregation and promote pDNA delivery in serum. J. Am. Chem. Soc. 128, 8176–8184.
Strand, S.P., Lelu, S., Reitan, N.K., Davies, C.L., Artursson, P., Vårum, K.M., 2010. Molecular design of chitosan gene delivery systems with an optimized balance between polyplex stability and polyplex unpacking. Biomaterials 31, 975–987.
Thakor, D.K., Teng, Y.D., Tabata, Y., 2009. Neuronal gene delivery by negatively charged pullulan–spermine/DNA anioplexes. Biomaterials 30, 815–1826.
Thibault, M., Nimesh, S., Lavertu, M., Buschmann, M.D., 2010. Intracellular trafficking and decondensation kinetics of chitosan–pDNA polyplexes. Mol. Ther., 1–8.
Tian, F., Hu, Y.L.K., Zhao, B., 2003. The depolymerisation mechanism of chitosan by hydrogen peroxide. J. Mater. Sci. 38, 4709–4712.
Vasir, J.K., Labhasetwar, V., 2007. Biodegradable nanoparticles for cytosolic delivery of therapeutics. Adv. Drug Deliv. Rev. 59, 718–728.
Verma, I.M., Somia, N., 1997. Gene therapy-promises, problems and prospects. Nature 389, 239–242.
Wu, Y., Liu, C., Zhao, X., Xiang, J., 2008. A new biodegradable polymer: PEGylated chitosan-g-PEI possessing a hydroxyl group at the PEG end. J. Polym. Res. 15, 181–185.
Yang, S.-J., Lin, F.-H., Tsai, K.-C., Wei, M.-F., Tsai, H.-M., Wong, J.-M., Shieh, M.-J., 2010. Folic acid-conjugated chitosan nanoparticles enhanced protoporphyrin IX accumulation in colorectal cancer cells. Bioconjug. Chem. 21, 679–689.
Zhang, Y., Yang, Y., Tang, K., Hu, X., Zou, G., 2008. Physicochemical characterization and antioxidant activity of quercetin-loaded chitosan nanoparticles. J. Appl. Polym. Sci. 107, 891–897.